Numerical Investigation of The Mobilization of Active Earth Pressure on Retaining Walls

Enquête numérique de la mobilisation de la pression de la terre active sur les murs de retenue

Sadrekarimi A., Damavandinejad Monfared S.
Western University, Department of Civil and Environmental Engineering, Spencer Engineering Building, London, Ontario, Canada. N6A 5B9.

ABSTRACT: The correct estimate of lateral earth pressure is important for the design of earth retaining structures. This study presents an investigation into the lateral earth pressure distribution on a wall and in particular the effect of arching at deeper levels of backfill for both at-rest and active conditions. Three-dimensional numerical simulations are performed using the ABAQUS finite element software. The effect of wall displacement, wall-backfill interaction, subsoil-wall interaction, subsoil-backfill interaction, soil modulus and friction angle on the mobilization of an active condition are investigated. The results of these simulations indicate that the true lateral stress distribution on a wall is non-linear and backfill arching increases by wall displacement and backfill-subsoil friction while increasing friction between the backfill and wall or subsoil and wall has no substantial effect on arching. The results are further compared with those from physical model tests. An active state is mobilized at wall displacements smaller than those suggested by Terzaghi's physical model tests. By increasing backfill-subsoil friction and backfill stiffness, the active state is mobilized at smaller wall displacements.

RÉSUMÉ: L'estimation correcte de la pression latérale des terres est importante pour la conception de structures de soutènement. Cette étude présente une étude sur la distribution de la pression latérale des terres sur un mur et en particulier l'effet d'arche en partie inférieure du remblai à la fois au repos et en poussée. Des simulations tridimensionnelles numériques sont réalisées en utilisant le logiciel ABAQUS d'éléments finis. L'effet du déplacement de la paroi, de l'interaction mur - remblai, de l'interaction sol-mur, du module du sol et de l'angle de frottement sur la mobilisation de la poussée sont étudiés. Les résultats de ces simulations montrent que la distribution réelle des contraintes latérales sur un mur est non linéaire et que l'effet d'arche dans le remblai augmente avec le déplacement de la paroi et le frottement entre remblai et sous-sol, alors que l'augmentation du frottement entre le remblai et le mur ou le sous-sol et le mur n'a pas d'effet substantiel sur cet effet d'arche. Les résultats sont ensuite comparés avec ceux d'essais sur modèles physiques. Un état de poussée est mobilisé pour des déplacements inférieurs à ceux suggérés par les essais de Terzaghi sur des modèles physiques. En augmentant le frottement entre le sous-sol et le remblai et la raideur du remblai, l'état actif est mobilisé pour des déplacements de la paroi plus petits.

KEYWORDS: finite element, retaining wall, active earth pressure, arching, displacement, numerical modeling.

1 INTRODUCTION

Estimating lateral earth pressure has been one of the earliest concerns in civil engineering and designing retaining structures. The most widely used theories of earth pressure are those of Coulomb (1776) and Rankine (1857) that are both based on the limit equilibrium theory. These classical methods have been used widely because of their simplicity. However, they provide little information regarding the distribution and magnitude of lateral earth pressures produced by different magnitudes of wall displacement. These methods are only valid for the limiting condition of sufficient ground and wall movements to mobilize an active state and do not provide any information for the conditions prior to the active state. Thus, several experimental (Terzaghi 1934; Sherif et al. 1984) and numerical (Clough and Duncan 1991; Mei et al. 2009; Salman et al. 2010) studies have been performed in order to evaluate the contributions of these factors on the lateral earth pressure distribution. This study presents a finite element numerical modeling investigation of the lateral earth pressure distribution and impact of wall displacement, wall-backfill interaction, subsoil-backfill interaction, backfill modulus and internal friction angle on the mobilization of an active condition. The numerical modeling results are then compared with experimental data of Terzaghi (1934) and Sherif et al. (1984).

2 NUMERICAL MODELING

Analyses are carried out using the ABAQUS finite element code. A model is developed for a 3 m wide by 10 m high retaining wall with plane strain boundary conditions that are chosen to minimize container boundary effects on the backfill sand. The wall and soil are modeled using 3D solid elements. The concrete wall is modeled as an elastic material using a linear isotropic elastic model. The extended Drucker-Prager plasticity model is used with a non-associated flow rule in this study for non-linear analyses of the backfill sand behavior. The parameters of this model are based on triaxial compression tests on Ottawa quartz sand (Sadrekarimi 2009). A non-dilatant flow is assumed ($\psi = 0$) to model a loose backfill sand. The choice of zero dilatancy angle was selected based on the extensive experimental experiences of the first author. For loose contractive sands (for which their state lies above the critical state line), the mobilized friction angle becomes equal to the critical state friction angle or in other words there is no negative or positive dilatancy angle (Manzari and Dafalias 1997; Been and Jefferies 2004). Accordingly, since our analyses simulate a loose contractive backfill, we use the critical state friction angle (32^o) with zero dilatancy to model the loose backfill.The properties of the backfill/foundation soil and wall are summarized in Table 1.

Table 1. Properties of the backfill/foundation soil and wall material

	γ (kN/m^3)	E (MPa)	ν	φ(◦)	ψ(◦)
Soil	14.4	115	0.3	32	0
Concrete wall	24.0	30,000[1]	0.2	-	-

[1] a very large Young's modulus (E) is assigned to the wall to model a stiff concrete retaining wall that does not deform under the applied backfill soil stresses.

Tangential and normal interactions at backfill-wall, and backfill-subsoil interfaces are taken into account using surface-to-surface contact interaction with surface-to-surface discretization method to enforce an overall contact condition over regions nearby slave nodes rather than only at individual slave nodes. A finite-sliding formulation is used at these interfaces, which allows any arbitrary motion of the surfaces including separation, sliding and rotation of the surfaces. A hard contact model is used to define the normal contact pressure-overclosure relationship between the wall (master) and the backfill (slave). Tangential interaction between the wall and the backfill is defined using the static-kinetic exponential decay function. A geostatic stress field procedure, in which gravity loads are applied, is used as the first step of the analysis to verify that the initial geostatic stress field is in equilibrium with applied loads and boundary conditions. The analysis is followed by a number of static analysis stages to reach an active state.

3 NUMERICAL RESULTS.

The vertical stress distributions behind the wall at an at-rest condition (Δ = 0.000H) and at different wall movements (Δ) are presented in Figure 1. According to this figure, vertical stress distribution becomes non-linear and decreases with wall depth (from the linear stress distribution) and increasing wall displacement. We anticipate that this non-linearity is produced by the arching of the backfill soil (within the failure wedge) between the wall and the backfill outside of the failure wedge. Arching is developed by the relative displacement at the interface of the backfill failure wedge and the backfill outside of the failure wedge. Without any wall movement, there is no relative displacement and therefore no arching or vertical stress reduction. As demonstrated later, backfill arching significantly affects lateral stress distribution on the wall.

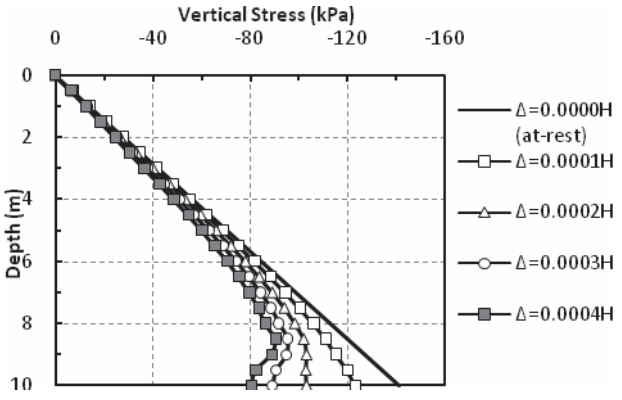

Figure 1: Vertical stress distributions behind the wall for different amounts of wall displacement (Δ)

Figure 2 presents the horizontal stress distributions at an at-rest condition and at different wall movements (Δ) as well as that from the Coulomb's theory. These are calculated for a model wall with a wall-backfill interface friction angle (δ_{wb}) of 20^o, wall-subsoil interface friction angle (δ_{ws}) of 15^o, and backfill-subsoil interface friction angle (δ_{sb}) of 32^o. The finite element pressure distribution diagram for Δ = 0.000H matches the at-rest stress diagram with a horizontal stress coefficient of 0.47 (based on K_o = 1 – sin 32^o from Jaky 1944). The finite element results indicate that the horizontal stress distribution behind a wall becomes non-linear with wall movement. As illustrated in Figure 1, with increasing wall displacement, backfill soil arching also increases and the total lateral trust (area of the horizontal stress distribution diagram) decreases. Furthermore, although the horizontal stress distribution diagrams almost converge for Δ ≥ 0.0003H, they are very different from the horizontal stress distribution diagram produced by Coulomb's method as this method does not take into account the effect of backfill soil arching. Despite this limitation, the total horizontal thrust from Coulomb's method is close to that obtained from the finite element analysis.

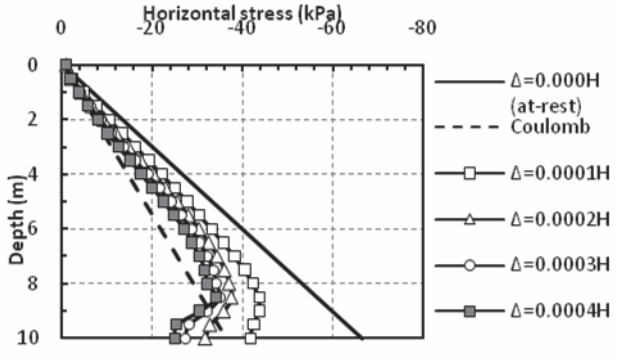

Figure 2: Horizontal stress distributions at different wall displacements as well as that from Coulomb's method for a wall with δ_{sb} = 32^o,δ_{ws} = 15^o and δ_{wb} = 20^o

In Figure 3, lateral stress distribution for models with different δ_{sb} values are presented at a wall movement of Δ = 0.0001H. The results show that the influence of arching increases by increasing δ_{sb}. This is produced by the backfill-subsoil interaction. At δ_{sb} = 5^o there is very little resistance from the subsoil and thus the backfill outside of the failure wedge follows the movement of the failure wedge, thus reducing soil arching. With increasing δ_{sb} the backfill is restrained from horizontal movement, the relative displacement between the backfill failure wedge and the backfill outside of the failure wedge increases, and thus arching and lateral stress reduction increase.

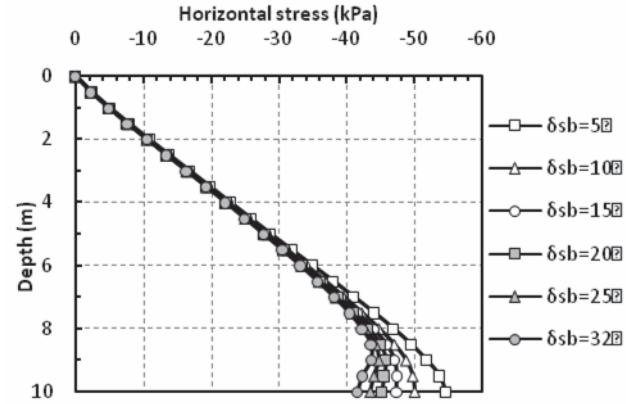

Figure 3: Lateral stress distributions for models with δ_{ws} = 15^o , δ_{wb} = 20^o, and with different magnitudes of δ_{sb}

Lateral stress reduction by arching is presented in Figures 4, 5 and 6 for different magnitudes of δ_{sb} , δ_{wb} and δ_{sw} respectively in models with different wall movements. These figures illustrate that the influence of backfill sand arching on lateral

stress reduction increases with increasing wall displacement and δ_{sb} whereas δ_{wb} and δ_{sw} have no substantial effect on arching. Figure 4 clearly indicates that there is no effect of backfill soil arching for $\delta_{sb} = 0^o$ and $\Delta = 0.0000H$ conditions. Thus, Coulomb's method could be considered as a special case for which $\delta_{sb} = 0^o$. However, $\Delta = 0.0000H$ (absolute at-rest condition) may not be practically possible as any yielding wall would slightly move during construction and backfilling, causing significant horizontal stress reduction. According to Figure 4, for a backfill and subsoil of the same sand ($\varphi' = \delta_{sb}$) a horizontal stress reduction of at least 30% is a prudent assumption (as $\varphi' \approx 30^o$ - 34^o for most sandy soils).

The influence of soil arching on lateral stress reduction is quantified as the ratio of $(p_a - p_i)$ to p_i, in which p_a is the lateral stress at wall's base that includes the effect of soil arching and p_i is the lateral stress that would have developed without any backfill soil arching. p_i is obtained by the linear extension of the lateral stress distribution curve down to wall's base.

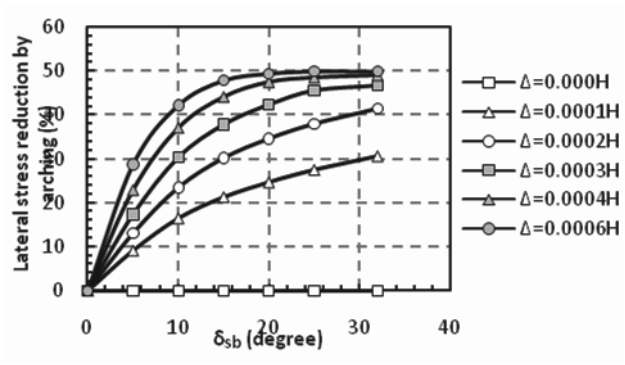

Figure 4: Arching-induced lateral stress reduction for $\delta_{wb} = 20^o$ at different magnitudes of wall translation and δ_{sb}

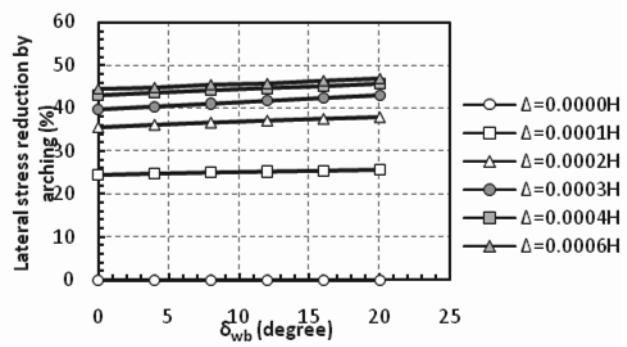

Figure 5: Arching-induced lateral stress reduction for $\delta_{sb} = 32^o$ and $\delta_{sw} = 15^o$ at different magnitudes of wall translation and δ_{wb}

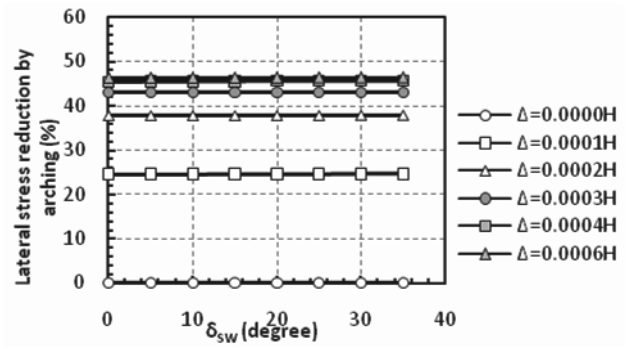

Figure 6: Arching-induced lateral stress reduction for $\delta_{sb} = 32^o$ and $\delta_{wb} = 20^o$ at different magnitudes of wall movement and δ_{sw}

Figures 7 and 8 show the influence of δ_{sb} and backfill soil modulus (E) on lateral stress reduction and the mobilization of an active state with wall movement (Δ), respectively. Lateral stress reduction is characterized by the ratio of the horizontal earth pressure coefficient at a particular wall movement, $K(\Delta/H)$ to the at-rest horizontal pressure coefficient (K_o). $K(\Delta/H)$ is obtained by normalizing total lateral thrust by $\gamma H^2/2$. By increasing δ_{sb}, the rate and the magnitude of horizontal earth pressure reduction significantly increase and converge for $\delta_{sb} > 5^o$. The effect of wall movement (Δ/H) on horizontal stress reduction is most significant for $\Delta/H < 0.0005$, after which it levels off as an active condition is mobilized. An active state ($K(\Delta/H)/K_o \approx 0.61$) is reached at smaller Δ/H as δ_{sb} increases, or in other words a greater δ_{sb} would limit the amount of wall movement required to reach an active failure state in the backfill soil. Figure 8 illustrates that the mobilization of an active failure condition is fairly independent of backfill soil modulus.

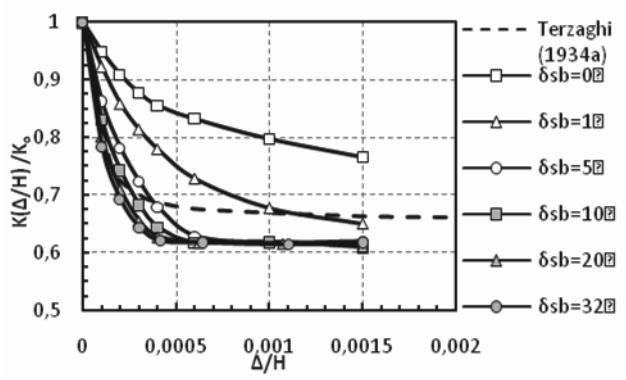

Figure. 7: Effect of wall movement and δ_{sb} on $K(\Delta/H)/K_o$ for retaining walls with $\delta_{wb} = 20^o$and $\delta_{sw} = 15^o$

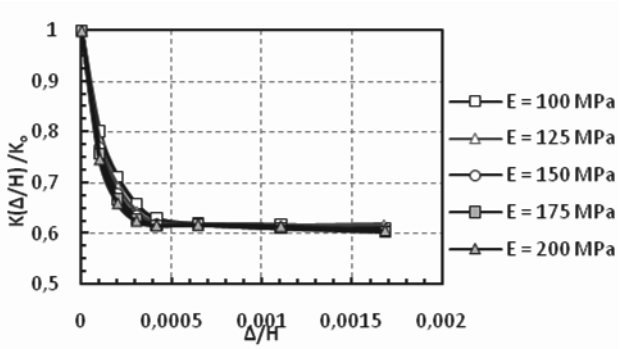

Figure 8: Effect of wall movement and backfill modulus (E) on $K(\Delta/H)/K_0$ for retaining walls with $\delta_{wb} = 20^o$, $\delta_{sw} = 15^o$ and $\delta_{sb} = 32^o$

The influence of soil's friction angle on the mobilization of an active state is presented in Figure 9. The results show that the amount of displacement that is required to mobilize an active state is independent of soil's internal friction angle which agrees with findings from physical model experiments (Sherif et al 1984). The results further show that the active horizontal earth pressure coefficient decreases by increasing soil's friction angle.

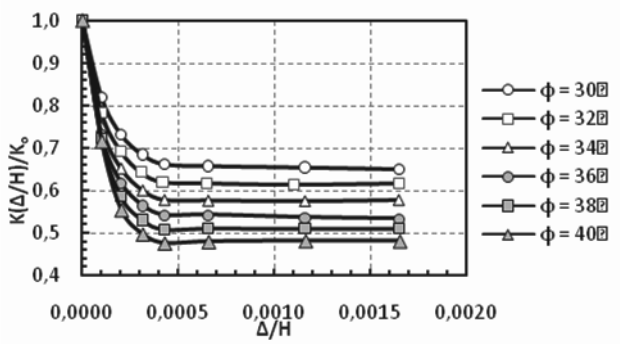

Figure 9: Effect of wall movement and soil's friction angle (φ) on $K(\Delta/H)/K_0$ for retaining walls with $\delta_{wb} = 20^o$, $\delta_{sw} = 15^o$ and $\delta_{sb} = 32^o$

In Figure 10, the impact of δ_{wb} on the mobilization of an active state with wall movement is presented. While the results show that increasing wall friction leads to reduced lateral stresses, there is no substantial effect on the amount of wall displacement required to mobilize an active condition. Similar to Figure 7, an active failure condition is mobilized at about Δ = 0.0004H.

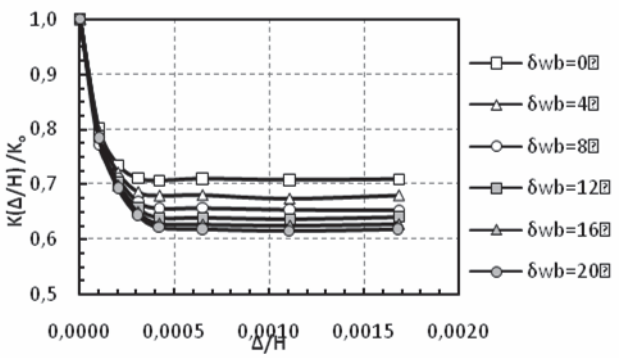

Figure 10: Effect of wall movement and δ_{wb} on the mobilization of $K(\Delta/H)/K_0$ for retaining walls with $\delta_{sb} = 32^o$ and $\delta_{sw} = 15^o$

4 COMPARISON WITH PHYSICAL MODEL TESTS

Figure 11 compares the finite element analyses of this study with the lateral earth pressures from physical model tests (Terzaghi 1934; Sherif et al. 1984). Comparisons are made with Sherif et al. (1984) results at the depths of soil pressure gages SP5 (depth/wall height = 0.22) and SP4 (depth/wall height = 0.38), whereas the lateral earth pressure coefficient from the overall earth pressure diagram is used for presenting Terzaghi (1934) data. Note that the lateral stresses from the finite element analyses are for walls moving horizontally, while Terzaghi (1934) and Sherif et al. (1984) experiments were conducted on walls rotating about their base. Accordingly, wall displacement (Δ) corresponds to the displacement measured at wall's mid-height for Terzaghi (1934) experiments, and is calculated from the amount of wall rotation at the corresponding depths for Sherif et al. (1984) experiments.

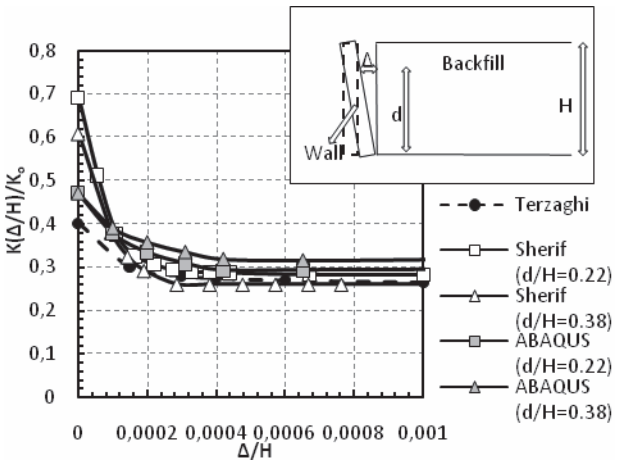

Figure 11: Effect of wall movement on horizontal stress reduction and the mobilization of an active condition based on the numerical analyses of this study and the experiments of Terzaghi (1934) and Sherif et al. (1984)

According to Figure 11, lateral stresses and their rate of reduction decrease with wall displacement in all studies. However, the initial rate of lateral stress reduction is the largest in Sherif et el. (1984) experiments, followed by the finite element analyses and Terzaghi's experiments. As a result, the active state is reached at smaller displacements (Δ = 0.0003H) in Sherif et al.'s experiments, followed by Δ = 0.0004H in the finite element analyses, and Terzaghi's experiments at Δ = 0.001H – 0.002H. These displacement are smaller than that (Δ = 0.004H) suggested by Clough and Duncan (1991) for reaching an active state in loose sands. Although the active stresses are more-or-less similar in all studies, the initial lateral stress coefficients are broadly different, which could likely be due to differences in backfill soil density and friction angle. Note that both Sherif et al. (1984) and Terzaghi (1934) report linear distributions for the active stress diagrams behind walls rotating about their base. While the effect of backfill soil arching is discussed in this study, we suspect that the difference in wall's mode of movement (rotation versus horizontal movement) could be the reason for not seeing arching in the physical model tests.

5 CONCLUSIONS

In this paper, the lateral earth pressure acting on a rigid retaining wall was studied using the finite element analysis method. The results of the simulations showed that the true earth pressure distribution is non-linear mainly due to soil arching effect at deeper levels and backfill-subsoil interaction to a lesser extent. The results indicated that the influence of backfill arching increases with wall displacement and backfill subsoil friction while increasing friction between the backfill and wall or subsoil and wall has no substantial effect on arching. The results were compared with those from physical model tests of Terzaghi (1934) and Sherif et al (1984). The results of these simulations showed that an active state is mobilized at wall displacements smaller than those suggested by the Terzaghi's physical model experiments but larger than those suggested by Sherif et al. (1984). The outcomes of this study further indicate that by increasing backfill-subsoil friction, the active state becomes mobilized at smaller wall displacements. The results also showed that although increasing wall-backfill interface friction leads to reduced lateral stresses, this has no effect on the wall displacement required to mobilize an active condition.

6 REFERENCES

ABAQUS Users Manual, version 6.10. 2010. Hibbitt, Karlsson and Sorenson Inc., Pawtucket, R.I.

Been, K., and Jefferies, M. (2004). "Stress-dilatancy in very loose sand." Canadian Geotechnical Journal, 41: 972 – 989.

Clough, G.W. and Duncan, J.M. 1991. Earth pressures. *Foundation engineering handbook*. 2nd ed. (H.Y. Fang, ed.) Van Nostrand Reinhold, New York, NY. pp. 223 - 235.

Coulomb, C.A. 1776. Essai sur une application des re`gles des maximis et minimis a` quelques proble`mes de statique relatifs a` l'architecture. In *Me`moires Acade`mie Royale Pre`sente´s par Divers Savants*, Paris. Vol. 7, pp. 343–382.

Jaky, J. 1944. The Coefficient of Earth Pressure at Rest. *Journal of the Society of Hungarian Architects and Engineers*, Budapest, Hungary, pp. 355.

Manzari, M.T., and Dafalias, Y.F. 1997. A critical state two-surface plasticity model for sands. Géotechnique, 47(2): 255–272.

Mei, G. Chen, Q. and Song, L. 2009. Model for predicting displacement-dependent lateral earth pressure. *Can. Geotech. J.* 46: 969–975 (2009).

Rankine, W.J.M. 1857. On the stability of loose earth. *Philosophical Transactions of the Royal Society of London*, 147(1 January): 9–27.

Sadrekarimi, A. 2009. Development of a new ring shear apparatus for investigating the critical state of sands. *Ph.D. Thesis, University of Illinois, Urbana-Champaign.*

Salman, F.A. Al-Shakarchi, Y.J. Husain, H.M. and Sabre, D.K., 2010. Distribution of earth pressure behind retaining walls considering different approaches. *International Journal of the Physical Sciences* Vol. 5(9), pp. 1389-1400.

Sherif, M.A. Fang, Y.S. and Sherif, R.I. 1984. Ka and K_0 behind rotating and non-yielding walls. *Journal of Geotechnical Engineering*, 110(1): 41–56.

Terzaghi, K. 1934. Large retaining-wall tests: I – Pressure of dry sand. *Engineering News–Record*, 85(1 February): 136–140.